entropy

MDPI

Article

Two Dynamical Scenarios for Binned Master Sample Interpretation

Giovanni Montani [1,2,*], Elisa Fazzari [2,3,4], Nakia Carlevaro [1] and Maria Giovanna Dainotti [5,6,7]

[1] Nuclear Department, ENEA, C.R. Frascati, Via E. Fermi 45, 00044 Frascati, Italy; nakia.carlevaro@enea.it
[2] Physics Department, "Sapienza" University of Rome, P.le A. Moro 5, 00185 Roma, Italy; elisa.fazzari@uniroma1.it
[3] Istituto Nazionale di Fisica Nucleare (INFN), Sezione di Roma, P.le A. Moro 5, 00185 Roma, Italy
[4] Physics Department, Tor Vergata University of Rome, Via della Ricerca Scientifica 1, 00133 Roma, Italy
[5] Division of Science, National Astronomical Observatory of Japan, 2-21-1, Mitaka 181-8588, Tokyo, Japan; maria.dainotti@nao.ac.jp
[6] Astronomy Department, The Graduate University for Advanced Studies (SOKENDAI), Shonankokusaimura, Hayama, Miura 240-0115, Kanagawa, Japan
[7] Space Science Institutes, 4765 Walnut St Ste B, Boulder, CO 80301, USA
* Correspondence: giovanni.montani@enea.it

Abstract

We analyze two different scenarios for the late universe dynamics, resulting in Hubble parameters deviating from the ΛCDM, mainly for the presence of an additional free parameter, which is the dark energy parameter. The first model consists of a pure evolutionary dark energy paradigm as a result of its creation by the gravitational field of the expanding universe. The second model also considers an interaction of the evolutionary dark energy with the matter component, postulated via the conservation of the sum of their ideal energy–momentum tensors. These two models are then compared via the diagnostic tool of the effective running Hubble constant, with the binned data of the so-called "Master sample" for the Type Ia Supernovae. The comparison procedures, based on a standard MCMC analysis, lead to a clear preference of data for the dark energy–matter interaction model, which is associated with a phantom matter equation of state parameter (very close to -1) when, being left free by data (it has a flat posterior), it is fixed in order to reproduce the decreasing power-law behavior of the effective running Hubble constant, already discussed in the literature.

Keywords: dark energy; late universe; supernovae

Academic Editor: Kazuharu Bamba

Received: 18 July 2025
Revised: 19 August 2025
Accepted: 20 August 2025
Published: 24 August 2025

Citation: Montani, G.; Fazzari, E.; Carlevaro, N.; Dainotti, M.G. Two Dynamical Scenarios for Binned Master Sample Interpretation. *Entropy* **2025**, *27*, 895. https://doi.org/10.3390/e27090895

1. Introduction

The emergence of a 4σ discrepancy between the measurement of the Hubble constant [1,2] by the SH0ES and Planck collaborations, refs. [3,4] referred to as Hubble tension, led the community to reconsider the ΛCDM model as the only viable cosmological dynamics for the late Universe evolution [3,5–37]. This tension is further emphasized by several other independent and model-independent determinations of H_0, distinct from SNe Ia calibrated with Cepheids (see [38] for a review). These include measurements based on SNe Ia calibrated with the tip of the red giant branch (TRGB) [39–41], galaxy distances using the Tully–Fisher relation (TFR) [42,43], Active Galactic Nuclei (AGN) [44], Gravitational Waves (GWs) and Dark Sirens [45–49], strong lensing time delays [50,51], Type II Supernovae [52], Megamasers [53], and Surface Brightness Fluctuations [54].

A fundamental step regarding the reliability of the ΛCDM model has been achieved by the DESI collaboration [55,56], which demonstrated how the redshift profile of their Baryonic Acoustic Oscillation (BAO) data is better fitted by a Chavellier–Polarski–Linder (CPL) model [57,58], also dubbed the w_0w_aCDM scenario. This result de facto stated convincing evidence for an evolutionary dark energy component across the late universe (see also [59–66]). However, the DESI collaboration, while partially solving the tension between the BAO and Cosmic Microwave Background (CMB) data, left entirely open the question of calibration based on the acoustic sound horizon and that of SH0ES, using Cepheids as standard candles [3]. The resulting picture, emerging from the last ten years of cosmological studies, is rather confused, and it suggests that new physical effects must be included in the late universe dynamics in order for it to take a consistent shape when combining different sources belonging to different redshift regions.

In [67,68], see also [69,70], these considerations led to investigating whether, in the same Type Ia Supernovae (SNe Ia) redshift distribution, an effective dependence of the Hubble constant on the considered binned representation can arise. In fact, a phenomenological power-law decreasing behavior has been detected as a better fit to binned data with respect to the ΛCDM model. The power-law behavior seen in the H_0 could be due either to the dynamical evolving dark energy model or to the $f(R)$ theory of gravity (see [12] and also [71]), but it could also account for selection biases, which are hidden due to different statistical assumptions (see [72]) and could be due to the evolution of the parameters of the SNe Ia (see [73]), the tip of the red giant brach stars [74], and of GRBs [75].

2. Theoretical Furmulation

Here, we perform a study based on two different models, which are then compared with the binned data of the so-called "Master sample" [69], in analogy to the study in [70]. The first scenario is based on an evolutionary dark energy formulation, which evolves with the redshift because it is created by the background gravitational field of the expanding universe [15,70,76–78] (for a detailed discussion see [Schiavone et al., "Revisiting the Matter-Creation Process: Constraints from Late-Time Acceleration and the Hubble Tension", in preparation]), according to a phenomenological ansatz for the produced particle rate, slightly modified with respect to the studies in [79,80] (actually we propose a mixed version of the two rates discussed in these papers, respectively). The second model is a revised version of the previous one, but with a completely different physical picture. In fact, the dark energy is still created by the gravitational field, but now it also interacts with the universe matter component via the condition that the sum of their energy–momentum tensors is conserved, instead of treating them separately (for other approaches with deformed matter contribution with respect to the ΛCDM model, see [81]). After testing these two models with the binned Master sample, we compare their predictions, especially in comparison to the ΛCDM dynamics and the power-law scaling, respectively.

The general scenario for developing the late universe models is a flat isotropic picture [82,83], whose line element reads as

$$ds^2 = -dt^2 + a^2(t)dl^2 \,, \tag{1}$$

where t denotes the synchronous time, dl^2 is the Euclidean infinitesimal distance, and $a(t)$ is the cosmic scale factor, regulating the expansion of the universe. The cosmological dynamics is driven by a (cold dark ρ_{dm} and baryonic ρ_b) matter energy density $\rho_m = \rho_{dm} + \rho_b$ and a dark energy contribution, with energy density ρ_{de} (we neglect here the radiation energy density, to be restored when investigating the dynamics up to the recombination era). Hence, the Friedmann equation is stated as follows:

$$H^2(t) \equiv \left(\frac{\dot{a}}{a}\right)^2 = \frac{\chi}{3}(\rho_m(t) + \rho_{de}(t)) \,, \tag{2}$$

where the dot refers to differentiation with respect to t and χ denotes the Einstein constant.

In the first proposed model, we retain the matter contribution ρ_m in its standard form, i.e., governed by the dynamics $\dot{\rho}_m(t) + 3H\rho_m(t) = 0$, which provides

$$\rho_m(z) = \rho_{m0}(1+z)^3 \,, \tag{3}$$

where, here and in the whole paper, we denote with the subscript 0 the present-day value of a quantity, and we have introduced the redshift variable $z \equiv 1/a - 1$ (we set equal to unity the present-day scale factor value). As a modification with respect to the standard ΛCDM model, we consider a process of dark energy creation by the (time-varying) gravitational field of the expanding universe, which is assumed to take place at equilibrium. Under these hypotheses, the continuity equation for the dark energy density reads as follows:

$$\dot{\rho}_{de}(t) = -3H(t)(1+w_{de})\left(1 - \frac{\Gamma(H,\rho_{de})}{3H(t)}\right)\rho_{de}(t) \,, \tag{4}$$

where Γ is the particle creation rate [79,80,84]. Above, w_{de} is the dark energy parameter and it is a free parameter of the model, subject to the constraint $w_{de} < -1/3$. In general, the phenomenological function $\Gamma(H,\rho_{de})$ is taken as a power-law of its own arguments [76,79]. In this respect, here, we consider the following *ansatz*:

$$\Gamma(H,\rho_{de}) = \Gamma^* H \rho_{de}^{-\alpha} \,, \tag{5}$$

where Γ^* and α are positive constants. We consider in the rate expression a linear term in H, stating, at highest order, the role of time-varying gravity in creating particles. We also add a dependence of Γ on a negative power of the dark energy density to suppress particle creation when its energy density increases.

Introducing the normalization $\Omega_{de} \equiv \chi\rho_{de}/3H_0^2$, where H_0 denotes the Hubble constant, Equation (4) can be rewritten as

$$\Omega'_{de}(z) = 3(1+w_{de})\left(1 - \bar{\Gamma}\,\Omega_{de}^{-\alpha}\right)\Omega_{de}/(1+z) \,, \tag{6}$$

where the prime indicates differentiation with respect to the redshift z and we have defined $\bar{\Gamma} = (\Gamma^*/3)(\chi/3H_0^2)^\alpha$. Furthermore, accordingly defining $\Omega_{m0} = \chi\rho_{m0}/3H_0^2$, the Friedmann equation Equation (2), via Equation (3), stands as follows:

$$E^2(z) \equiv \left(\frac{H}{H_0}\right)^2 = \Omega_{m0}(1+z)^3 + \Omega_{de}(z) \,, \tag{7}$$

with $E(z)$ denoting the universe expansion rate. Thus we get the following initial condition $\Omega_{de}(0) = 1 - \Omega_{m0}$, and Equation (6) now admits the following solution:

$$\Omega_{de}(z) = \left[\bar{\Gamma} + ((1-\Omega_{m0})^\alpha - \bar{\Gamma})\,(1+z)^{3(1+w_{de})\alpha}\right]^{1/\alpha} . \tag{8}$$

We finally get, associated with our first model, the following Hubble parameter:

$$H(z) = H_0\sqrt{\Omega_{m0}(1+z)^3 + \left[\bar{\Gamma} + ((1-\Omega_{m0})^\alpha - \bar{\Gamma})(1+z)^{3(1+w_{de})\alpha}\right]^{1/\alpha}} . \tag{9}$$

This evolutionary dark energy model generalizes the ΛCDM dynamics, and it contains five free parameters, i.e., H_0, Ω_{m0}, $\bar{\Gamma}$, α, and w_{de}. It is immediately recognizable that the Hubble

parameter in Equation (9) reduces to the standard ΛCDM one when we require $w_{de} = -1$. Finally, it is easy to realize that for $z > 1$ the $H(z)$ is very weakly sensitive to the values taken by the parameter α, and, in what follows, we will address the simplest case $\alpha = 1$. It is worth noting that, in this case, the effective equation of state for the dark energy is associated, in $z = 0$, to the following parameter w_0^{eff}:

$$w_0^{eff} = -1 + (1 + w_{de})\left(1 - \frac{\bar{\Gamma}}{\Omega_{de}(0)}\right). \tag{10}$$

Now we require that, today, the intrinsic nature of dark energy, traced by w_{de}, remains the same, quintessence or phantom, also for the effective equation of state, dictated by w_0^{eff}. To this end, we have to require the constraint $\bar{\Gamma}\Omega_{de}(0) < 1$. Since the value of $\Omega_{de}(0)$ is expected (see also the concordance hypothesis [4]) close to the value 0.7, in what follows, we will consider for $\bar{\Gamma}$ the reference value 0.5.

Let us now introduce the diagnostic tool, corresponding to the effective running Hubble constant with the redshift $\mathcal{H}_0(z)$ (see [67–71]), i.e.,

$$\mathcal{H}_0(z) \equiv \frac{H(z)}{\sqrt{\Omega_m^0(1+z)^3 + 1 - \Omega_m^0}}, \tag{11}$$

which, in the analyzed case $\alpha = 1$, takes the following form:

$$\mathcal{H}_0(z) \equiv H_0\sqrt{\frac{\Omega_m^0(1+z)^3 + \bar{\Gamma} + (1 - \Omega_m^0 - \bar{\Gamma})(1+z)^{3(1+w_{de})}}{\Omega_m^0(1+z)^3 + 1 - \Omega_m^0}}. \tag{12}$$

Before moving to the data analysis, let us now introduce an alternative version of dynamics, our second model, in which the matter and the dark energy interact and the latter is still created by the gravitational field of the expanding universe (for other interaction mechanisms and related reviews, see [85–111]). The interaction between these two basic components is phenomenologically described by requiring that the sum of the matter ideal energy–momentum tensor $T_{\mu\nu}^{(m)}$ and that of dark energy $T_{\mu\nu}^{(de)}$ is conserved instead of the separated standard laws; i.e., we require that the following relation holds:

$$\nabla_\nu\left(T_\mu^{(m)\nu} + T_\mu^{(de)\nu}\right) = 0\,. \tag{13}$$

Defining $\Omega \equiv \Omega_m + \Omega_{de}$, in the case of the considered flat isotropic universe, the relation above can be restated via the following continuity equation:

$$\Omega'(z) = (3\Omega(z) + 3w_{de}\Omega_{de}(z))/(1+z)\,, \tag{14}$$

where by construction $\Omega(0) = 1$, while retaining the same process of dark energy present in Equation (6), now takes the simplified form

$$\Omega'_{de}(z) = -3(1 + w_{de})\bar{\Gamma}\Omega_{de}(z)^{1-\alpha}/(1+z)\,, \tag{15}$$

with the same relation $\Omega_{de}(0) = 1 - \Omega_{m0}$. This equation admits now the solution

$$\Omega_{de}(z) = \left[(1 - \Omega_{m0})^\alpha - 3\alpha(1 + w_{de})\bar{\Gamma}\ln(1+z)\right]^{1/\alpha}, \tag{16}$$

providing an alternative form of the dark energy component evolution. Clearly, the first equation using (15) can be explicitly rewritten for the matter component as

$$\Omega'_m(z) = 3\Omega_m(1+z)^{-1} + 3(1 + w_{de})\Omega_{de}(1+z)^{-1}(1 + \bar{\Gamma}\Omega_{de}^{-\alpha})\,. \tag{17}$$

Finally, we can write the following alternative effective Hubble constant:

$$\tilde{\mathcal{H}}_0(z) = H_0 \sqrt{\frac{\Omega}{\Omega_m^0 (1+z)^3 + 1 - \Omega_m^0}}\,, \tag{18}$$

associated with the equation for Ω in correspondence with the expression for Ω_{de}. Also in this case, we deal with the simplest case $\alpha = 1$. Despite the fact that in the present scenario the value $\bar{\Gamma} = 0.5$ is no longer essential to ensure that the effective equation of state parameter today has the same signature as the intrinsic one w_{de}, we still preserve this reference choice to better compare the two physical cases, without and with dark energy–matter interaction, respectively.

3. Data Analysis

We now perform a statistical analysis of these two models, labeled as DE and DE-DM, respectively, in order to find the free parameters of the models (H_0, Ω_{m_0}, and w_{de}) that optimize the probability of finding the data we use. In particular, we compare the theoretical expressions of the effective running Hubble constant in Equations (12) and (18) with data from the *Master binned SNe Ia sample* [69], which is a compilation of SNe Ia from DESy5 [112], JLA [113], Pantheon+ [19,21], and Pantheon [20] without duplicates. We use this dataset, selecting the 20 equally populated bin combination, as performed in [70]. The entire catalog covers redshifts from 0.00122 to 2.3. The mean redshift of the first bin is 0.0091, while that of the last bin is 1.54. This sample was originally fitted with a power-law (PL) function of the form $\mathcal{H}_0(z) = \frac{H_0}{(1+z)^a}$, yielding best-fit parameters $a = 0.010$ and $H_0 = 69.869$ km/s/Mpc. Both [69,70] have shown that this phenomenological function is preferred over ΛCDM, wCDM, and a reduced version of the w_0w_aCDM model. This dataset is hereafter referred to as the "Master bin." The uniform priors used in this work are $H_0 = \mathcal{U}[60, 80]$, $\Omega_{m_0} = \mathcal{U}[0.01, 0.99]$, and $w_{de} = \mathcal{U}[-3, 1]$.

We perform the statistical analysis by sampling the posterior distribution using the Monte Carlo Markov Chain (MCMC) method implemented in the publicly available `Cobaya` software (3.5.5 version) [114]. Convergence of the chains is determined using the Gelman–Rubin criterion, requiring $R - 1 < 0.01$ [115]. Statistical results and graphs are produced with the `GetDist` tool (1.6.1 version) [116]. Specifically, we use a preliminary version of a code that will be publicly released in a forthcoming work [Giarè, Fazzari, in prep.].

To compare the models, we evaluate the differences in the Bayesian Information Criterion (BIC) [117] for the tested model with respect to the PL parametrization, which we adopt as the reference. This difference is defined as $\Delta\text{BIC} = \text{BIC}_i - \text{BIC}_{\text{PL}}$. To interpret the strength of the evidence, we use Jeffreys' scale [118–120], which categorizes support against a model as inconclusive for $0 < |\Delta\text{BIC}| < 1$, weak for $1 < |\Delta\text{BIC}| < 2.5$, moderate for $2.5 < |\Delta\text{BIC}| < 5.0$, and strong for $|\Delta\text{BIC}| > 5.0$. Notably, negative values of ΔBIC indicate a preference for the tested model over the PL parametrization.

4. Results

Table 1 and Figure 1 present the results of our analysis. These findings indicate that the Master binned data sample can effectively constrain the dark energy parameter w_{de} only in the DE model, while w_{de} remains unconstrained in the DE-DM model.

This fact corresponds to the possibility of setting this parameter with a specific additional phenomenological requirement without compromising the predictive power of the data analysis. In our case, we fix its value by imposing the significant requirement that our Hubble parameter provides a statistically meaningful representation of the power-law discussed in [69,70]. To this end, we extract from the PL profile, reconstructed by the

best-fit values recorded above, 100 points used to minimize the residuals of the two curves (resulting in residuals less than 0.15%). As a result of this procedure, we determine the value of $w_{de} = -1.0073$, outlining a weak phantom nature of the dark energy. Furthermore, for the DE model we find $\Delta\text{BIC} = 6.6$, suggesting that the DE model is strongly disfavored compared to the PL case.

Table 1. Mean values and associated uncertainties for the parameters inferred from the MCMC analysis for the DE and DE-DM models.

Model	H_0 [km s^{-1} Mpc^{-1}]	Ω_{m_0}	w_{de}
DE	69.872 ± 0.080	0.3246 ± 0.0053	-1.052 ± 0.058
DE-DM	69.959 ± 0.064	0.3084 ± 0.0037	–

Figure 2 shows the reconstruction of the running Hubble constant for the two theoretical models, using the following best-fit values:

$$\text{DE}: \quad H_0 = 69.872, \quad \Omega_{m_0} = 0.3240, \quad w_{de} = -1.049\,, \tag{19}$$

$$\text{DE} - \text{DM}: \quad H_0 = 69.959, \quad \Omega_{m_0} = 0.3086, \quad w_{de} = -1.007. \tag{20}$$

These values are obtained by minimizing the χ^2 statistic resulting from the MCMC analysis. For the DE model, we follow the standard procedure and we obtain the values shown in Equation (19). In the DE-DM model, since the MCMC analysis does not effectively constrain w_{de}, we fix it to the value obtained from the PL fit profile discussed earlier and then determine the best-fit values of the remaining parameters by performing a new MCMC analysis with w_{de} held fixed.

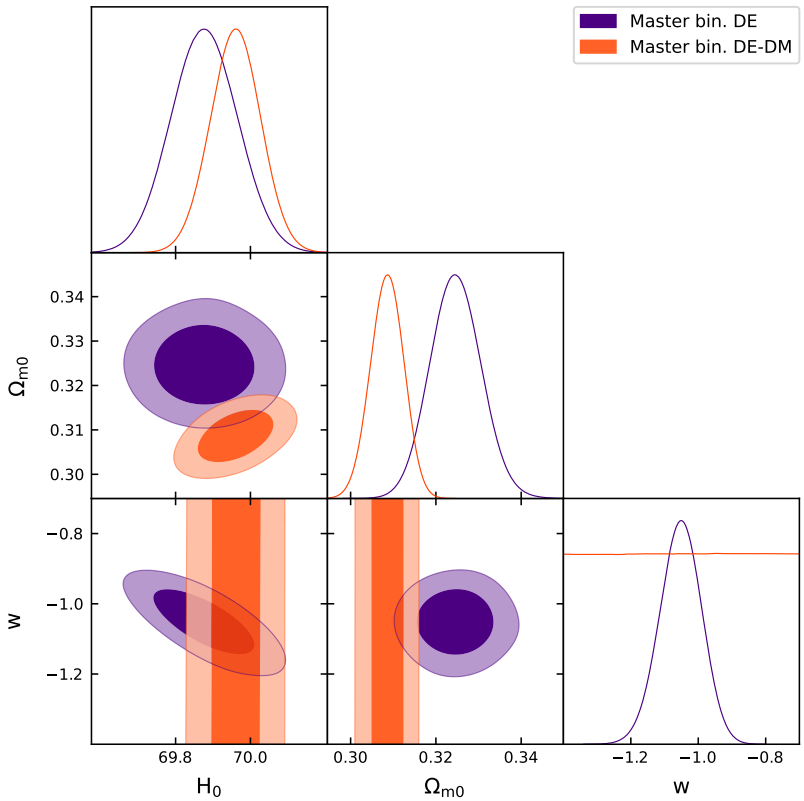

Figure 1. One-dimensional posterior probability distributions and two-dimensional 68% and 95% CL contours on cosmological parameters of the DE and DE-DM models obtained using the Master binned sample.

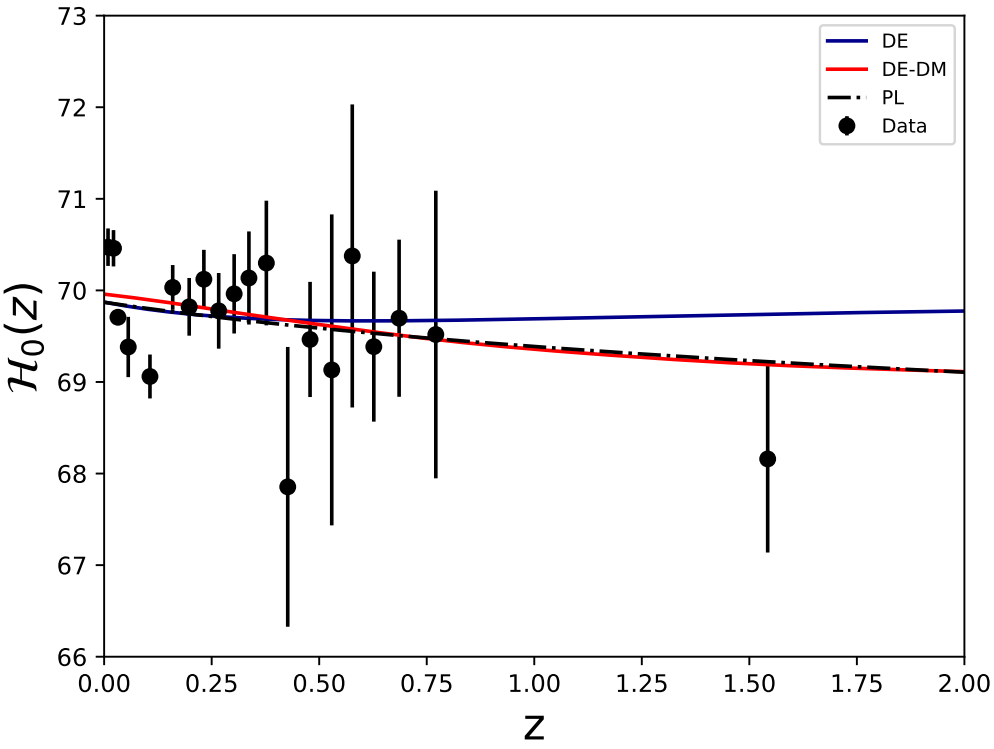

Figure 2. Reconstruction of the effective running Hubble constant for the DE model, DE-DM model, and the PL reference model. We adopted the best-fit values shown in Equations (19) and (20).

5. Conclusions

In summary, we analyzed two different reformulations of the late universe dynamics, both deviating from the ΛCDM scenario: the first model is based on pure evolutionary dark energy, in which it is created by the cosmological gravitational field; the second picture relies on dark energy–matter interaction, described via the conservation law of the sum of the two energy–momentum tensors, while dark energy now varies just by virtue of its gravitational creation. The process of dark energy creation is driven by the rate of constituent production, which is proportional to the Hubble parameter and to the inverse of the dark energy density itself: the idea we propose here is that the (non-stationary) expanding universe is able to create particles, but this process is weaker as the created energy density increases. The comparison of the two models with the 20-bin data of the Master sample led to interesting results about how SNe Ia data alone can constrain the late universe dynamics. The comparison of the pure evolutionary dark energy model with binned data allowed us to establish that the corresponding phenomenology is not very appropriate to describe observations: actually the fit of the binned data suggested that this scenario is disfavored with respect to the power-law decreasing behavior, discussed in [70].

This result is consistent with the idea that the evolutionary dark energy scenario is essential to properly interpret the DESI collaboration data [55,56], but it has a limited impact on the behavior of the $\mathcal{H}_0(z)$, see [67–69], which is expected to be related to the Hubble tension itself. The second model outlined a very different feature, since the MCMC procedure is unable to constraint the value of the dark energy parameter w_{de}. This fact suggests that the value of such a parameter does not impact, in the proposed scenario, the capability of the model to fit data. Nonetheless, this degree of freedom can be used to constraint the $\mathcal{H}_0(z)$ to be a very good representation of the power-law decay observed in [69] when the binned Master sample is concerned. This result is of particular relevance because it shows how, like the metric $f(R)$ scenario discussed in [12], dark energy interact-

ing with matter is a good paradigm to reproduce a monotonically decreasing behavior of the phenomenologically observed values of H_0.

The explanation of this similarity consists of the dominant role acquired by the matter term. If the matter term decreases with respect to a standard ΛCDM model (nonetheless the dark energy component is growing as in a quintessence scenario), soon or later, we should observe a global decreasing rescaling of $\mathcal{H}_0(z)$, which is, in this respect, very similar to the corresponding global decreasing rescaling due to the non-minimally coupled scalar field of the $f(R)$ model in the Jordan frame, as outlined in [11,12].

We can conclude that the analysis of the present manuscript reinforces the idea that the interaction of the matter and dark energy components of the universe is a very promising scenario in which we could accommodate, on one hand, the evidence from the DESI collaboration observations and, on the other hand, the tension that such data generate with the SH0ES collaboration [21] versus the SNe Ia calibration [19,20], the latter effect being mainly driven by an altered matter contribution with respect to the ΛCDM paradigm.

Author Contributions: Conceptualization, G.M.; methodology, G.M., E.F., N.C., and M.G.D.; software, E.F. and N.C.; validation, E.F. and N.C.; formal analysis, G.M., N.C., and E.F.; investigation, G.M. and N.C.; resources, M.G.D.; data curation, E.F. and M.G.D.; writing—original draft preparation, G.M., E.F., and N.C.; writing—review and editing, G.M., E.F., N.C., and M.G.D.; visualization, E.F. All authors have read and agreed to the published version of the manuscript.

Funding: This research received no external funding.

Institutional Review Board Statement: Not applicable.

Data Availability Statement: The original contributions presented in this study are included in the article; further inquiries can be directed to the corresponding author.

Acknowledgments: Author E. Fazzari is supported by "Theoretical Astroparticle Physics" (TAsP), iniziativa specifica INFN. E.F. acknowledges the IT Services at The University of Sheffield for providing high-performance computing resources. M.G. Dainotti acknowledges the support of the DoS and is also grateful for the support by the JSPS Grant-in-Aid for Scientific Research (KAKENHI) (A), Grant Number JP25H00675.

Conflicts of Interest: The authors declare no conflicts of interest.

References

1. de Bernardis, P.; Ade, P.A.R.; Bock, J.J.; Bond, J.R.; Borrill, J.; Boscaleri, A.; Coble, K.; Crill, B.P.; De Gasperis, G.; Farese, P.C.; et al. A flat Universe from high-resolution maps of the cosmic microwave background radiation. *Nature* **2000**, *404*, 955–959. [CrossRef]
2. Bennett, C.L.; Larson, D.; Weiland, J.L.; Jarosik, N.; Hinshaw, G.; Odegard, N.; Smith, K.M.; Hill, R.S.; Gold, B.; Halpern, M.; et al. Nine-year Wilkinson Microwave Anisotropy Probe (WMAP) Observations: Final Maps and Results. *Astrophys. J. Suppl. Ser.* **2013**, *208*, 20. [CrossRef]
3. Riess, A.G.; Yuan, W.; Macri, L.M.; Scolnic, D.; Brout, D.; Casertano, S.; Jones, D.O.; Murakami, Y.; Anand, G.S.; Breuval, L.; et al. A comprehensive measurement of the local value of the Hubble constant with 1 km s^{-1} Mpc-1 uncertainty from the Hubble Space Telescope and the SH0ES team. *Astrophys. J. Lett.* **2022**, *934*, L7. [CrossRef]
4. Aghanim, N.; Akrami, Y.; Ashdown, M.; Aumont, J.; Baccigalupi, C.; Ballardini, M.; Banday, A.J.; Barreiro, R.; Bartolo, N.; Basak, S.; et al. Planck 2018 results-VI. Cosmological parameters. *Astron. Astrophys.* **2020**, *641*, A6.
5. Di Valentino, E.; Levi Said, J.; Riess, A.; Pollo, A.; Poulin, V.; Gómez-Valent, A.; Weltman, A.; Palmese, A.; Huang, C.D.; Carsten, v.d.B.; et al. The CosmoVerse White Paper: Addressing observational tensions in cosmology with systematics and fundamental physics. *Phys. Dark Universe* **2025**, *49*, 101965. [CrossRef]
6. Di Valentino, E.; Mena, O.; Pan, S.; Visinelli, L.; Yang, W.; Melchiorri, A.; Mota, D.F.; Riess, A.G.; Silk, J. In the realm of the Hubble tension—A review of solutions. *Class. Quantum Gravity* **2021**, *38*, 153001. [CrossRef]
7. Vagnozzi, S. Seven hints that early-time new physics alone is not sufficient to solve the Hubble tension. *Universe* **2023**, *9*, 393. [CrossRef]
8. Escamilla, L.A.; Fiorucci, D.; Montani, G.; Di Valentino, E. Exploring the Hubble tension with a late time Modified Gravity scenario. *Phys. Dark Universe* **2024**, *46*, 101652. [CrossRef]

9. Montani, G.; Carlevaro, N.; Escamilla, L.A.; Di Valentino, E. Kinetic model for dark energy—dark matter interaction: Scenario for the hubble tension. *Phys. Dark Universe* **2025**, *48*, 101848. [CrossRef]
10. Montani, G.; Carlevaro, N.; Dainotti, M.G. Slow-rolling scalar dynamics as solution for the Hubble tension. *Phys. Dark Universe* **2024**, *44*, 101486. [CrossRef]
11. Montani, G.; De Angelis, M.; Bombacigno, F.; Carlevaro, N. Metric $f(R)$ gravity with dynamical dark energy as a scenario for the Hubble tension. *Mon. Not. R. Astron. Soc. Lett.* **2023**, *527*, L156–L161. [CrossRef]
12. Schiavone, T.; Montani, G.; Bombacigno, F. f(R) gravity in the Jordan frame as a paradigm for the Hubble tension. *Mon. Not. R. Astron. Soc. Lett.* **2023**, *522*, L72–L77. [CrossRef]
13. Schiavone, T.; Montani, G.; Dainotti, M.G.; De Simone, B.; Rinaldi, E.; Lambiase, G. Running Hubble constant from the SNe Ia Pantheon sample? In Proceedings of the 17th Italian-Korean Symposium on Relativistic Astrophysics, Gunsan, Republic of Korea, 2–6 August 2021.
14. Nojiri, S.; Odintsov, S.D. Introduction to modified gravity and gravitational alternative for dark energy. *eConf* **2007**, *4*, 115–145. [CrossRef]
15. Silva, E.; Sabogal, M.A.; Scherer, M.; Nunes, R.C.; Di Valentino, E.; Kumar, S. New constraints on interacting dark energy from DESI DR2 BAO observations. *Phys. Rev. D* **2025**, *111*, 123511. [CrossRef]
16. Teixeira, E.M.; Giarè, W.; Hogg, N.B.; Montandon, T.; Poudou, A.; Poulin, V. Implications of distance duality violation for the H_0 tension and evolving dark energy. *arXiv* **2025**, arXiv:2504.10464.
17. Giarè, W. Inflation, the Hubble tension, and early dark energy: An alternative overview. *Phys. Rev. D* **2024**, *109*, 123545. [CrossRef]
18. Anderson, R.I.; Koblischke, N.W.; Eyer, L. Small-amplitude Red Giants Elucidate the Nature of the Tip of the Red Giant Branch as a Standard Candle. *Astrophys. J. Lett.* **2024**, *963*, L43. [CrossRef]
19. Scolnic, D.; Brout, D.; Carr, A.; Riess, A.G.; Davis, T.M.; Dwomoh, A.; Jones, D.O.; Ali, N.; Charvu, P.; Chen, R.; et al. The Pantheon+ Analysis: The Full Data Set and Light-curve Release. *Astrophys. J.* **2022**, *938*, 113. [CrossRef]
20. Scolnic, D.M.; Jones, D.O.; Rest, A.; Pan, Y.C.; Chornock, R.; Foley, R.J.; Huber, M.E.; Kessler, R.; Narayan, G.; Riess, A.G.; et al. The Complete Light-curve Sample of Spectroscopically Confirmed SNe Ia from Pan-STARRS1 and Cosmological Constraints from the Combined Pantheon Sample. *Astrophys. J.* **2018**, *859*, 101. [CrossRef]
21. Brout, D.; Scolnic, D.; Popovic, B.; Riess, A.G.; Carr, A.; Zuntz, J.; Kessler, R.; Davis, T.M.; Hinton, S.; Jones, D.; et al. The Pantheon+ Analysis: Cosmological Constraints. *Astrophys. J.* **2022**, *938*, 110. [CrossRef]
22. Scolnic, D.; Riess, A.G.; Wu, J.; Li, S.; Anand, G.S.; Beaton, R.; Casertano, S.; Anderson, R.I.; Dhawan, S.; Ke, X. CATS: The Hubble Constant from Standardized TRGB and Type Ia Supernova Measurements. *Astrophys. J. Lett.* **2023**, *954*, L31. [CrossRef]
23. Jones, D.O.; Mandel, K.S.; Kirshner, R.P.; Thorp, S.; Challis, P.M.; Avelino, A.; Brout, D.; Burns, C.; Foley, R.J.; Pan, Y.-C.; et al. Cosmological Results from the RAISIN Survey: Using Type Ia Supernovae in the Near Infrared as a Novel Path to Measure the Dark Energy Equation of State. *Astrophys. J.* **2022**, *933*, 172. [CrossRef]
24. Anand, G.S.; Tully, R.B.; Rizzi, L.; Riess, A.G.; Yuan, W. Comparing Tip of the Red Giant Branch Distance Scales: An Independent Reduction of the Carnegie-Chicago Hubble Program and the Value of the Hubble Constant. *Astrophys. J.* **2022**, *932*, 15. [CrossRef]
25. Freedman, W.L. Measurements of the Hubble Constant: Tensions in Perspective. *Astrophys. J.* **2021**, *919*, 16. [CrossRef]
26. Uddin, S.A.; Burns, C.R.; Phillips, M.M.; Suntzeff, N.B.; Freedman, W.L.; Brown, P.J.; Morrell, N.; Hamuy, M.; Krisciunas, K.; Wang, L.; et al. Carnegie Supernova Project-I and -II: Measurements of H_0 using Cepheid, TRGB, and SBF Distance Calibration to Type Ia Supernovae. *arXiv* **2023**, arXiv:2308.01875.
27. Huang, C.D.; Yuan, W.; Riess, A.G.; Hack, W.; Whitelock, P.A.; Zakamska, N.L.; Casertano, S.; Macri, L.M.; Marengo, M.; Menzies, J.W.; et al. The Mira Distance to M101 and a 4% Measurement of H_0. *Astrophys. J.* **2024**, *963*, 83. [CrossRef]
28. Li, S.; Riess, A.G.; Casertano, S.; Anand, G.S.; Scolnic, D.M.; Yuan, W.; Breuval, L.; Huang, C.D. Reconnaissance with JWST of the J-region Asymptotic Giant Branch in Distance Ladder Galaxies: From Irregular Luminosity Functions to Approximation of the Hubble Constant. *Astrophys. J.* **2024**, *966*, 20. [CrossRef]
29. Kourkchi, E.; Tully, R.B.; Anand, G.S.; Courtois, H.M.; Dupuy, A.; Neill, J.D.; Rizzi, L.; Seibert, M. Cosmicflows-4: The Calibration of Optical and Infrared Tully–Fisher Relations. *Astrophys. J.* **2020**, *896*, 3. [CrossRef]
30. Schombert, J.; McGaugh, S.; Lelli, F. Using the Baryonic Tully–Fisher Relation to Measure H_0. *Astron. J.* **2020**, *160*, 71. [CrossRef]
31. Murakami, Y.S.; Riess, A.G.; Stahl, B.E.; Kenworthy, W.D.; Pluck, D.M.A.; Macoretta, A.; Brout, D.; Jones, D.O.; Scolnic, D.M.; Filippenko, A.V. Leveraging SN Ia spectroscopic similarity to improve the measurement of H_0. *J. Cosmol. Astropart. Phys.* **2023**, *11*, 046. [CrossRef]
32. Breuval, L.; Riess, A.G.; Casertano, S.; Yuan, W.; Macri, L.M.; Romaniello, M.; Murakami, Y.S.; Scolnic, D.; Anand, G.S.; Soszyński, I. Small Magellanic Cloud Cepheids Observed with the Hubble Space Telescope Provide a New Anchor for the SH0ES Distance Ladder. *arXiv* **2024**, arXiv:2404.08038. [CrossRef]

33. Balkenhol, L.; Dutcher, D.; Mancini, A.S.; Doussot, A.; Benabed, K.; Galli, S.; Ade, P.A.R.; Anderson, A.J.; Ansarinejad, B.; Archipley, M.; et al. Measurement of the CMB temperature power spectrum and constraints on cosmology from the SPT-3G 2018 TT, TE, and EE dataset. *Phys. Rev. D* **2023**, *108*, 023510. [CrossRef]
34. Aiola, S.; Calabrese, E.; Maurin, L.; Naess, S.; Schmitt, B.L.; Abitbol, M.H.; Addison, G.E.; Ade, P.A.R.; Alonso, D.; Amiri, M.; et al. The Atacama Cosmology Telescope: DR4 Maps and Cosmological Parameters. *J. Cosmol. Astropart. Phys.* **2020**, *12*, 047. [CrossRef]
35. Foidl, H.; Rindler-Daller, T. A proposal to improve the accuracy of cosmological observables and address the Hubble tension problem. *Astron. Astrophys.* **2024**, *686*, A210. [CrossRef]
36. Luongo, O.; Muccino, M. Determining H_0 from distance sum rule combining gamma-ray bursts with observational Hubble data and strong gravitational lensing. *arXiv* **2024**, arXiv:2412.18493. [CrossRef]
37. Shah, R.; Mukherjee, P.; Saha, S.; Garain, U.; Pal, S. Deep Learning Based Recalibration of SDSS and DESI BAO Alleviates Hubble and Clustering Tensions. *arXiv* **2024**, arXiv:2412.14750. [CrossRef]
38. Verde, L.; Treu, T.; Riess, A.G. Tensions between the early and late Universe. *Nat. Astron.* **2019**, *3*, 891–895. [CrossRef]
39. Freedman, W.L.; Madore, B.F.; Hatt, D.; Hoyt, T.J.; Jang, I.S.; Beaton, R.L.; Burns, C.R.; Lee, M.G.; Monson, A.J.; Neeley, J.R.; et al. The Carnegie-Chicago Hubble Program. VIII. An Independent Determination of the Hubble Constant Based on the Tip of the Red Giant Branch. *Astrophys. J.* **2019**, *882*, 34. [CrossRef]
40. Freedman, W.L.; Madore, B.F.; Hoyt, T.; Jang, I.S.; Beaton, R.; Lee, M.G.; Monson, A.; Neeley, J.; Rich, J. Calibration of the Tip of the Red Giant Branch (TRGB). *arXiv* **2020**, arXiv:2002.01550. [CrossRef]
41. Soltis, J.; Casertano, S.; Riess, A.G. The Parallax of ω Centauri Measured from Gaia EDR3 and a Direct, Geometric Calibration of the Tip of the Red Giant Branch and the Hubble Constant. *Astrophys. J. Lett.* **2021**, *908*, L5. [CrossRef]
42. Watkins, R.; Allen, T.; Bradford, C.J.; Ramon, A.; Walker, A.; Feldman, H.A.; Cionitti, R.; Al-Shorman, Y.; Kourkchi, E.; Tully, R.B. Analysing the large-scale bulk flow using cosmicflows4: Increasing tension with the standard cosmological model. *Mon. Not. R. Astron. Soc.* **2023**, *524*, 1885–1892. [CrossRef]
43. Luković, V.V.; Haridasu, B.S.; Vittorio, N. Exploring the evidence for a large local void with supernovae Ia data. *Mon. Not. R. Astron. Soc.* **2020**, *491*, 2075–2087. [CrossRef]
44. Lu, W.J.; Qin, Y.P. New constraint of the Hubble constant by proper motions of radio components observed in AGN twin-jets. *Res. Astron. Astrophys.* **2021**, *21*, 261. [CrossRef]
45. Gerardi, F.; Feeney, S.M.; Alsing, J. Unbiased likelihood-free inference of the Hubble constant from light standard sirens. *arXiv* **2021**, arXiv:2104.02728. [CrossRef]
46. Gray, R.; Messenger, C.; Veitch, J. A Pixelated Approach to Galaxy Catalogue Incompleteness: Improving the Dark Siren Measurement of the Hubble Constant. *arXiv* **2021**, arXiv:2111.04629. [CrossRef]
47. Li, B.; Shapiro, P.R. Precision cosmology and the stiff-amplified gravitational-wave background from inflation: NANOGrav, Advanced LIGO-Virgo and the Hubble tension. *J. Cosmol. Astropart. Phys.* **2021**, *2021*, 024. [CrossRef]
48. Mozzon, S.; Ashton, G.; Nuttall, L.K.; Williamson, A.R. Does non-stationary noise in LIGO and Virgo affect the estimation of H_0? *arXiv* **2021**, arXiv:2110.11731.
49. Palmese, A.; Bom, C.R.; Mucesh, S.; Hartley, W.G. A standard siren measurement of the Hubble constant using gravitational wave events from the first three LIGO/Virgo observing runs and the DESI Legacy Survey. *arXiv* **2021**, arXiv:2111.06445. [CrossRef]
50. Zhu, S.; Shu, Y.; Yuan, H.; Fu, J.N.; Gao, J.; Wu, J.; He, X.; Liao, K.; Li, G.; Er, X.; et al. Forecast of Observing Time Delay of Strongly Lensed Quasars with the Muztagh-Ata 1.93 m Telescope. *Res. Astron. Astrophys.* **2023**, *23*, 035001. [CrossRef]
51. Liu, Y.; Oguri, M. Assessing the effect of mass-model assumptions on measuring the Hubble constant from the cluster-lensed supernova Refsdal. *Phys. Rev. D* **2025**, *111*, 123506. [CrossRef]
52. de Jaeger, T.; Galbany, L.; Riess, A.G.; Stahl, B.E.; Shappee, B.J.; Filippenko, A.V.; Zheng, W. A 5 per cent measurement of the Hubble-Lemaître constant from Type II supernovae. *Mon. Not. R. Astron. Soc.* **2022**, *514*, 4620–4628. [CrossRef]
53. Pesce, D.W.; Braatz, J.A.; Reid, M.J.; Riess, A.G.; Scolnic, D.; Condon, J.J.; Gao, F.; Henkel, C.; Impellizzeri, C.M.V.; Kuo, C.Y.; et al. The Megamaser Cosmology Project. XIII. Combined Hubble Constant Constraints. *Astrophys. J. Lett.* **2020**, *891*, L1. [CrossRef]
54. Blakeslee, J.P.; Jensen, J.B.; Ma, C.P.; Milne, P.A.; Greene, J.E. The Hubble Constant from Infrared Surface Brightness Fluctuation Distances. *Astrophys. J.* **2021**, *911*, 65. [CrossRef]
55. Adame, A.G.; Aguilar, J.; Ahlen, S.; Alam, S.; Alexander, D.M.; Alvarez, M.; Alves, O.; Anand, A.; Andrade, U.; Armengaud, E.; et al. DESI 2024 VI: Cosmological constraints from the measurements of baryon acoustic oscillations. *J. Cosmol. Astropart. Phys.* **2025**, *02*, 021. [CrossRef]
56. Abdul-Karim, M.; Aguilar, J.; Ahlen, S.; Alam, S.; Allen, L.; Prieto, C.A.; Alves, O.; Anand, A.; Andrade, U.; Armengaud, E.; et al. DESI DR2 Results II: Measurements of Baryon Acoustic Oscillations and Cosmological Constraints. *arXiv* **2025**, arXiv:2503.14738.
57. Chevallier, M.; Polarski, D. Accelerating universes with scaling dark matter. *Int. J. Mod. Phys. D* **2001**, *10*, 213–223. [CrossRef]
58. Linder, E.V. Exploring the expansion history of the universe. *Phys. Rev. Lett.* **2003**, *90*, 091301. [CrossRef] [PubMed]
59. Lodha, K.; Calderon, R.; Matthewson, W.; Shafieloo, A.; Ishak, M.; Pan, J.; Garcia-Quintero, C.; Huterer, D.; Valogiannis, G.; Ureña-López, L.; et al. Extended Dark Energy analysis using DESI DR2 BAO measurements. *arXiv* **2025**, arXiv:2503.14743.

60. Giarè, W.; Mahassen, T.; Di Valentino, E.; Pan, S. An overview of what current data can (and cannot yet) say about evolving dark energy. *Phys. Dark Universe* **2025**, *48*, 101906. [CrossRef]
61. Giarè, W. Dynamical Dark Energy Beyond Planck? Constraints from multiple CMB probes, DESI BAO and Type-Ia Supernovae. *arXiv* **2024**, arXiv:2409.17074. [CrossRef]
62. Giarè, W.; Najafi, M.; Pan, S.; Di Valentino, E.; Firouzjaee, J.T. Robust preference for Dynamical Dark Energy in DESI BAO and SN measurements. *J. Cosmol. Astropart. Phys.* **2024**, *2024*, 035. [CrossRef]
63. Colgáin, E.Ó.; Dainotti, M.G.; Capozziello, S.; Pourojaghi, S.; Sheikh-Jabbari, M.; Stojkovic, D. Does DESI 2024 Confirm ΛCDM? *arXiv* **2024**, arXiv:2404.08633. [CrossRef]
64. Ray, S.; Khlopov, M.; Ghosh, P.P.; Mukhopadhyay, U. Phenomenology of Λ-CDM Model: A Possibility of Accelerating Universe with Positive Pressure. *Int. J. Theor. Phys.* **2011**, *50*, 939–951. [CrossRef]
65. Dymnikova, I.; Khlopov, M. Decay of Cosmological Constant as Bose Condensate Evaporation. *Mod. Phys. Lett. A* **2000**, *15*, 2305–2314. [CrossRef]
66. Doroshkevich, A.G.; Khlopov, M.I. Formation of structure in a universe with unstable neutrinos. *Mon. Not. RAS* **1984**, *211*, 277–282. [CrossRef]
67. Dainotti, M.G.; De Simone, B.; Schiavone, T.; Montani, G.; Rinaldi, E.; Lambiase, G. On the Hubble constant tension in the SNe Ia Pantheon sample. *Astrophys. J.* **2021**, *912*, 150. [CrossRef]
68. Dainotti, M.G.; De Simone, B.; Schiavone, T.; Montani, G.; Rinaldi, E.; Lambiase, G.; Bogdan, M.; Ugale, S. On the evolution of the Hubble constant with the SNe Ia pantheon sample and baryon acoustic oscillations: A feasibility study for GRB-cosmology in 2030. *Galaxies* **2022**, *10*, 24. [CrossRef]
69. Dainotti, M.G.; Simone, B.D.; Garg, A.; Kohri, K.; Bashyal, A.; Aich, A.; Mondal, A.; Nagataki, S.; Montani, G.; Jareen, T.; et al. A New Master Supernovae Ia sample and the investigation of the H_0 tension. *arXiv* **2025**, arXiv:2501.11772.
70. Fazzari, E.; Dainotti, M.G.; Montani, G.; Melchiorri, A. The effective running Hubble constant in SNe Ia as a marker for the dark energy nature. *arXiv* **2025**, arXiv:2506.04162. [CrossRef]
71. Schiavone, T.; Montani, G. Evolution of an effective Hubble constant in $f(R)$ modified gravity. *arXiv* **2024**, arXiv:2408.01410.
72. Dainotti, M.G.; Bargiacchi, G.; Bogdan, M.; Capozziello, S.; Nagataki, S. On the statistical assumption on the distance moduli of Supernovae Ia and its impact on the determination of cosmological parameters. *J. High Energy Astrophys.* **2024**, *41*, 30–41. [CrossRef]
73. Nicolas, N.; Rigault, M.; Copin, Y.; Graziani, R.; Aldering, G.; Briday, M.; Kim, Y.L.; Nordin, J.; Perlmutter, S.; Smith, M. Redshift evolution of the underlying type Ia supernova stretch distribution. *Astron. Astrophys.* **2021**, *649*, A74. [CrossRef]
74. Freedman, W.L.; Madore, B.F.; Hoyt, T.J.; Jang, I.S.; Lee, A.J.; Owens, K.A. Status Report on the Chicago-Carnegie Hubble Program (CCHP): Measurement of the Hubble Constant Using the Hubble and James Webb Space Telescopes. *Astrophys. J.* **2025**, *985*, 203. [CrossRef]
75. Dainotti, M.G.; Lenart, A.Ł.; Chraya, A.; Sarracino, G.; Nagataki, S.; Fraija, N.; Capozziello, S.; Bogdan, M. The gamma-ray bursts fundamental plane correlation as a cosmological tool. *Mon. Not. R. Astron. Soc.* **2023**, *518*, 2201–2240. [CrossRef]
76. Elizalde, E.; Khurshudyan, M.; Odintsov, S.D. Can we learn from matter creation to solve the H_0 tension problem? *Eur. Phys. J. C* **2024**, *84*, 782. [CrossRef]
77. Fazzari, E.; Leo, C.D.; Montani, G.; Martinelli, M.; Melchiorri, A.; Cañas-Herrera, G. Investigating $f(R)$-Inflation: Background evolution and constraints. *arXiv* **2025**, arXiv:2507.13890.
78. Scherer, M.; Sabogal, M.A.; Nunes, R.C.; De Felice, A. Challenging ΛCDM: 5σ Evidence for a Dynamical Dark Energy Late-Time Transition. *arXiv* **2025**, arXiv:2504.20664. [CrossRef]
79. Calvao, M.; Lima, J.; Waga, I. On the thermodynamics of matter creation in cosmology. *Phys. Lett. A* **1992**, *162*, 223–226. [CrossRef]
80. Montani, G. Influence of particle creation on flat and negative curved FLRW universes. *Class. Quantum Gravity* **2001**, *18*, 193. [CrossRef]
81. Dainotti, M.G.; Lenart, A.; Yengejeh, M.G.; Chakraborty, S.; Fraija, N.; Di Valentino, E.; Montani, G. A new binning method to choose a standard set of Quasars. *Phys. Dark Universe* **2024**, *44*, 101428. [CrossRef]
82. Efstathiou, G.; Gratton, S. The evidence for a spatially flat Universe. *Mon. Not. R. Astron. Soc. Lett.* **2020**, *496*, L91–L95. [CrossRef]
83. Weinberg, S. *Gravitation and Cosmology: Principles and Applications of the General Theory of Relativity*; Wiley: Hoboken, NJ, USA, 1972.
84. Nunes, R.C.; Pavón, D. Phantom behavior via cosmological creation of particles. *Phys. Rev. D* **2015**, *91*, 063526. [CrossRef]
85. Amendola, L. Coupled quintessence. *Phys. Rev. D* **2000**, *62*, 043511. [CrossRef]
86. Bolotin, Y.L.; Kostenko, A.; Lemets, O.A.; Yerokhin, D.A. Cosmological evolution with interaction between dark energy and dark matter. *Int. J. Mod. Phys. D* **2015**, *24*, 1530007. [CrossRef]
87. Wang, B.; Abdalla, E.; Atrio-Barandela, F.; Pavón, D. Dark matter and dark energy interactions: Theoretical challenges, cosmological implications and observational signatures. *Rep. Prog. Phys.* **2016**, *79*, 096901. [CrossRef]

88. Wang, B.; Gong, Y.; Abdalla, E. Transition of the dark energy equation of state in an interacting holographic dark energy model. *Phys. Lett. B* **2005**, *624*, 141–146. [CrossRef]
89. Das, S.; Corasaniti, P.S.; Khoury, J. Superacceleration as the signature of a dark sector interaction. *Phys. Rev. D* **2006**, *73*, 083509. [CrossRef]
90. Pan, S.; Chakraborty, S. A cosmographic analysis of holographic dark energy models. *Int. J. Mod. Phys. D* **2014**, *23*, 1450092. [CrossRef]
91. Barrow, J.D.; Clifton, T. Cosmologies with energy exchange. *Phys. Rev. D* **2006**, *73*, 103520. [CrossRef]
92. Amendola, L.; Camargo Campos, G.; Rosenfeld, R. Consequences of dark matter-dark energy interaction on cosmological parameters derived from SNIa data. *Phys. Rev. D* **2007**, *75*, 083506. [CrossRef]
93. He, J.H.; Wang, B. Effects of the interaction between dark energy and dark matter on cosmological parameters. *J. Cosmol. Astropart. Phys.* **2008**, *2008*, 010. . [CrossRef]
94. Väliviita, J.; Majerotto, E.; Maartens, R. Large-scale instability in interacting dark energy and dark matter fluids. *J. Cosmol. Astropart. Phys.* **2008**, *2008*, 020. [CrossRef]
95. Yang, W.; Li, H.; Wu, Y.; Lu, J. Cosmological constraints on coupled dark energy. *J. Cosmol. Astropart. Phys.* **2016**, *2016*, 007. [CrossRef]
96. Majerotto, E.; Väliviita, J.; Maartens, R. Adiabatic initial conditions for perturbations in interacting dark energy models. *Mon. Not. R. Astron. Soc.* **2010**, *402*, 2344–2354. [CrossRef]
97. Väliviita, J.; Maartens, R.; Majerotto, E. Observational constraints on an interacting dark energy model. *Mon. Not. R. Astron. Soc.* **2010**, *402*, 2355–2368. [CrossRef]
98. Chimento, L.P. Linear and nonlinear interactions in the dark sector. *Phys. Rev. D* **2010**, *81*, 043525. [CrossRef]
99. He, J.H.; Wang, B.; Abdalla, E. Testing the interaction between dark energy and dark matter via the latest observations. *Phys. Rev. D* **2011**, *83*, 063515. [CrossRef]
100. Chimento, L.P.; Richarte, M.G. Interacting dark sector with transversal interaction. In *AIP Conference Proceedings*; AIP Publishing LLC: College Park, MD, USA, 2015; Volume 1647, pp. 44–49. [CrossRef]
101. Costa, A.A.; Xu, X.D.; Wang, B.; Ferreira, E.G.M.; Abdalla, E. Testing the interaction between dark energy and dark matter with Planck data. *Phys. Rev. D* **2014**, *89*, 103531. [CrossRef]
102. Yang, W.; Xu, L. Testing coupled dark energy with large scale structure observation. *J. Cosmol. Astropart. Phys.* **2014**, *2014*, 034. [CrossRef]
103. Nunes, R.C.; Pan, S.; Saridakis, E.N. New constraints on interacting dark energy from cosmic chronometers. *Phys. Rev. D* **2016**, *94*. [CrossRef]
104. D'Amico, G.; Hamill, T.; Kaloper, N. Quantum field theory of interacting dark matter and dark energy: Dark monodromies. *Phys. Rev. D* **2016**, *94*, 103526. [CrossRef]
105. Paliathanasis, A.; Pan, S.; Yang, W. Dynamics of nonlinear interacting dark energy models. *Int. J. Mod. Phys. D* **2019**, *28*, 1950161. [CrossRef]
106. Cheng, G.; Ma, Y.Z.; Wu, F.; Zhang, J.; Chen, X. Testing interacting dark matter and dark energy model with cosmological data. *Phys. Rev. D* **2020**, *102*, 043517. [CrossRef]
107. Zhai, Y.; Giarè, W.; van de Bruck, C.; Valentino, E.D.; Mena, O.; Nunes, R.C. A consistent view of interacting dark energy from multiple CMB probes. *J. Cosmol. Astropart. Phys.* **2023**, *2023*, 032. [CrossRef]
108. Johnson, J.P.; Sangwan, A.; Shankaranarayanan, S. Observational constraints and predictions of the interacting dark sector with field-fluid mapping. *J. Cosmol. Astropart. Phys.* **2022**, *2022*, 024. [CrossRef]
109. Kumar, S. Remedy of some cosmological tensions via effective phantom-like behavior of interacting vacuum energy. *Phys. Dark Universe* **2021**, *33*, 100862. [CrossRef]
110. Yang, W.; Pan, S.; Valentino, E.D.; Nunes, R.C.; Vagnozzi, S.; Mota, D.F. Tale of stable interacting dark energy, observational signatures, and the H0 tension. *J. Cosmol. Astropart. Phys.* **2018**, *2018*, 019. [CrossRef]
111. von Marttens, R.; Casarini, L.; Mota, D.; Zimdahl, W. Cosmological constraints on parametrized interacting dark energy. *Phys. Dark Universe* **2019**, *23*, 100248. [CrossRef]
112. Abbott, T.; Acevedo, M.; Aguena, M.; Alarcon, A.; Allam, S.; Alves, O.; Amon, A.; Andrade-Oliveira, F.; Annis, J. The Dark Energy Survey: Cosmology Results with 1500 New High-redshift Type Ia Supernovae Using the Full 5 yr Data Set. *Astrophys. J. Lett.* **2024**, *973*, L14. [CrossRef]
113. Betoule, M.; Kessler, R.; Guy, J.; Mosher, J.; Hardin, D.; Biswas, R.; Astier, P.; El-Hage, P.; Konig, M.; Kuhlmann, S.; et al. Improved cosmological constraints from a joint analysis of the SDSS-II and SNLS supernova samples. *Astron. Astrophys.* **2014**, *568*, A22. [CrossRef]
114. Torrado, J.; Lewis, A. Cobaya: Code for Bayesian Analysis of hierarchical physical models. *J. Cosmol. Astropart. Phys.* **2021**, *2021*, 057. [CrossRef]
115. Gelman, A.; Rubin, D.B. Inference from iterative simulation using multiple sequences. *Stat. Sci.* **1992**, *7*, 457–472. [CrossRef]

116. Lewis, A. GetDist: A Python package for analysing Monte Carlo samples. *arXiv* **2019**, arXiv:1910.13970. [CrossRef]
117. Wagenmakers, E.J. A Practical Solution to the Pervasive Problems of *p* Values. *Psychon. Bull. Rev.* **2007**, *14*, 779–804. [CrossRef]
118. Trotta, R. Bayes in the sky: Bayesian inference and model selection in cosmology. *Contemp. Phys.* **2008**, *49*, 71–104. [CrossRef]
119. Kass, R.E.; Raftery, A.E. Bayes factors. *J. Am. Stat. Assoc.* **1995**, *90*, 773–795. [CrossRef]
120. Jeffreys, H. *The Theory of Probability*; Oxford Classic Texts in the Physical Sciences; Oxford University Press: Oxford, UK, 1939.